Alternating Lamellar Structure of Triblock Copolymers of the ABA Type

Y. Matsushita,*,[1a] M. Nomura,[1b] J. Watanabe,[1c] Y. Mogi,[1d] and I. Noda

Department of Applied Chemistry, Nagoya University, Furo-cho, Chikusa-ku, Nagoya, 464-01 Japan

M. Imai

The Institute for Solid State Physics, Neutron Scattering Laboratory, University of Tokyo, Shirakata, Tokai, Naka, Ibaraki, 319-11 Japan

Received October 12, 1994; Revised Manuscript Received June 6, 1995[⊗]

ABSTRACT: Alternating lamellar structures of poly(2-vinylpyridine-*b*-styrene-*b*-2-vinylpyridine) triblock copolymers of the ABA type with different compositions were studied by transmission electron microscopy (TEM), small-angle X-ray scattering (SAXS), and small-angle neutron scattering (SANS). The volume fractions of polystyrene (S), ϕ_s, of the copolymers range from 0.28 to 0.58, whereas the chain lengths of two end block polymers, poly(2-vinylpyridine) (P), are always the same for each sample. It was confirmed that all the solvent-cast films had alternating lamellar structures, and the measured microdomain spacings were in good agreement with the theoretical prediction by Helfand and Wasserman irrespective of the compositions. SANS studies revealed that the middle block polymers (S) are elongated along the direction normal to the lamellar interface, but they are shrunk along the direction parallel to the interface, so that the volume occupied by the middle block polymers are the same as those in the unperturbed states, and the degree of deformation decreases with increasing ϕ_s.

Introduction

Microdomain structures of block copolymers have been extensively studied on diblock copolymers of the AB type,[2−5] so as to be understood at the molecular level. The alternating lamellar structure has been examined[6−13] more quantitatively than the other structures because they are geometrically the simplest and can be considered in equilibrium compared with the other structures, that is, spherical, cylindrical, and bicontinuous structures. In recent years, the chain conformations of block polymers in lamellar microdomains were measured for several polymers by SANS,[14−17] and it was found that the block chains were shrunk in the direction parallel to the domain interface so as to compensate for the elongation in the normal direction.

The most remarkable feature of the microdomain structures of ABA triblock copolymers is that they have middle block polymers (B) both ends of which must be anchored either on different domain boundaries or on the same boundary, while two A block polymers have free ends in microdomains. The former chain conformation for the middle block polymers can be called "bridge-type" conformation and the latter "loop-type". This feature contrasts significantly with that of diblock copolymers where both A and B block polymers have their own free ends.

The purpose of the present paper is to study the difference between the lamellar domain spacings, D, of diblock and triblock copolymers and also to study the dependence of chain conformation of middle block polymers on the composition in comparison with that of diblock copolymers, so that we can elucidate the contribution of the two types of conformations. Thus we prepared poly(2-vinylpyridine-*b*-styrene-*b*-2-vinylpyridine) (PSP) triblock copolymers and their deuterium-labeled counterparts as samples in this study.

Experimental Section

Samples were prepared by an anionic block copolymerization of styrene and 2-vinylpyridine monomers with the dipotassium salt of α-methylstyrene tetramer as a bifunctional initiator in tetrahydrofurane (THF) at −78 °C. Styrene-d_8 monomer was also used to prepare labeled block copolymer for SANS. Details of sample preparation and characterization will be described elsewhere.[18] Table 1 summarizes the molecular characteristics of samples for morphological studies, while Table 2 shows those of labeled and unlabeled copolymer pairs for SANS study.

Films for morphological observations were cast from dilute solutions of THF and annealed at 150 °C under vacuum for 4 days. Morphological observations were carried out by TEM and SAXS. *X-ray was irradiated from the direction parallel to the film surface (edge view), and a scintillation counter was swept along the direction transverse to lamellae so as to measure domain spacings (D) of the copolymers, because the lamellar microdomains are known to align predominantly parallel to the film surface. The details of SAXS measurements were described previously,[13] and the experimental condtiions of TEM observations will be reported elsewhere.*[18] SANS measurements were performed with the SANS-U spectrometer of the Institute for Solid State Physics (ISSP) of the University of Tokyo in JRR-3M at Tokai.[19] The wavelength λ used was 0.7 nm, and its distribution $\Delta\lambda/\lambda$ was 0.1. Sample to detector distances adopted were 4, 6, and 8 m, depending on the dimension of the polymers. SANS intensities were measured in two geometries, i.e., edge and through views, in which neutron beams are incident in the directions parallel and perpendicular to the film surface, respectively, as shown in Figure 1.

The composition-matching was examined to eliminate the domain scattering from the total coherent scattering intensity in the edge view for two blend samples, blends I and IV. Since the calculated ratio of poly(styrene-d_8) (D) to poly(styrene-h_8) (S), for matching the scattering length of the polystyrene blend to that of poly(2-VP), is 0.107/0.893 by volume,[20] several mixtures with different mixing ratios were prepared around this ratio for these two blends.

Results

Figure 2 shows typical examples of transmission electron micrographs of an unlabeled polymer, PSP-11,

[⊗] Abstract published in *Advance ACS Abstracts,* August 1, 1995.

0024-9297/95/2228-6007$09.00/0

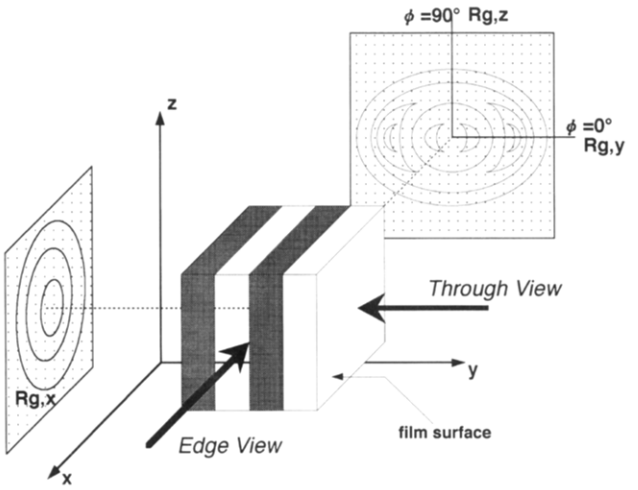

Figure 1. Schematic representation of SANS measurements.

Table 1. Molecular Characteristics of Triblock Copolymers for Morphological Studies

sample code	$10^{-4}M_n$ 2-VP	S	2-VP	M_w/M_n	ϕ_S
PSP-14	6.30	6.40	6.30	1.05	0.28
PSP-8	3.58	3.10	3.58	1.03	0.32
PSP-9	7.95	6.86	7.95	1.02	0.32
PSP-5	3.76	3.41	3.76	1.02	0.33
PSP-4	3.04	3.58	3.04	1.02	0.39
PSP-2	3.27	4.54	3.27	1.03	0.43
PSP-11	2.45	4.49	2.45	1.04	0.50
PSP-3	2.66	4.90	2.66	1.02	0.50
PSP-10	1.16	2.24	1.16	1.05	0.51
PSP-12	2.89	7.23	2.89	1.04	0.58

Table 2. Molecular Characteristics of Samples for SANS Study

blend code	sample code	$10^{-4}M_n$ 2-VP	S	2-VP	M_w/M_n	ϕ_S
I	PDP-1	3.00	2.96	3.00	1.02	0.34
	PSP-8	3.58	3.10	3.58	1.03	0.32
II	PDP-2	6.64	5.98	6.64	1.02	0.33
	PSP-9	7.95	6.86	7.95	1.02	0.32
III	PDP-4	1.15	2.00	1.15	1.02	0.49
	PSP-10	1.16	2.24	1.16	1.05	0.51
IV	PDP-5	2.30	4.25	2.30	1.03	0.50
	PSP-11	2.45	4.49	2.45	1.04	0.50
V	PDP-3	2.93	5.67	2.93	1.02	0.51
	PSP-3	2.66	4.90	2.66	1.02	0.50
VI	PDP-6	4.03	9.02	4.03	1.04	0.58
	PSP-12	2.89	7.23	2.89	1.04	0.55

and its blend with a labeled polymer, i.e., PDP-5/PSP-11. All the other samples with different compositions were also found to have alternating lamellar structures, though their micrographs are not shown here. Figure 3 shows the comparison between SAXS edge-view diffraction patterns of six samples. Integer order peaks can be seen for all patterns reflecting lamellar structures, though two of them are missing because of the particle scattering factors.[21] They are the second-order peak for PSP-3, where ϕ_s is about $^1/_2$ and the third-order one for PSP-5, where ϕ_s is approximately $^1/_3$. Microdomain spacings, D, were obtained by applying the Bragg conditions, $D = 2\pi n/q_p$, to the magnitude of wave vector q_p $(=4\pi\ (\sin)\ \theta)/\lambda)$ for integer order diffraction peaks, where 2θ is the scattering angle. They are plotted against the number-averaged molecular weight of copolymers M_n (○) together with the data of styrene-2-vinylpyridine (SP) diblock copolymers (△)[13] in Figure 4.

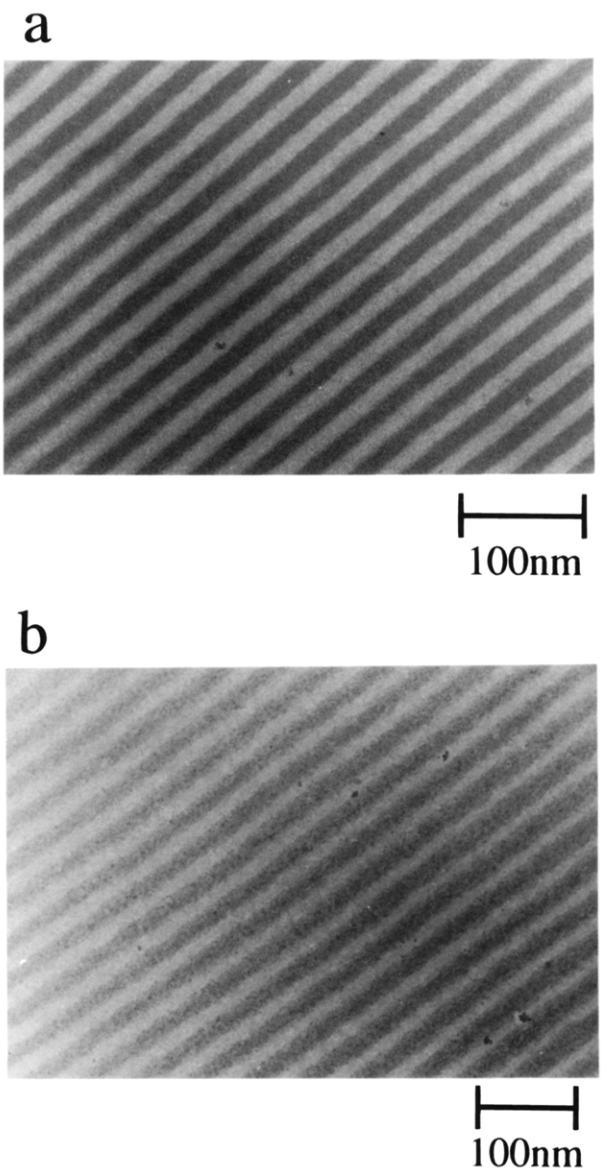

Figure 2. Electron micrographs showing the lamellar microphase-separated structure as examples: (a) PSP-11; (b) PDP-5/PSP-11 blend with a blend ratio of 10/90 by weight.

SANS measurement were also carried out in through the edge views. Figure 5 shows an example of a two-dimensional intensity map in the through view. Since neither diffraction nor anisotropy was observed in the through view, all the data were circularly-averaged. Figure 6a shows the circularly-averaged data for PDP-5/PSP-11 in the through view as an example, and Guinier plots of their coherent scattering intensities are shown in Figure 6b. The magnitude of errors propagated through background data correction procedures was shown by error bars for each data point. From the initial slope of this plot, we evaluated the radii of gyration of polystyrenes in the direction parallel to the lamellar interface[17] assuming that the orientation of lamellae is perfect. Fitting to straight lines was carried out by taking respective uncertainties into account. The values of statistical errors were also added to each component of the radii of gyration. Though the coordinates x and z are equivalent in Figure 1, we define the component of the radius of gyration obtained from the through-view data as $R_{g,x}$ for simplicity.[17] Table 3 lists $R_{g,x}$ thus obtained for PDP/PSP blends together with the uncertainties with different ϕ_s's. This table also lists the unperturbed radii of gyration $R_{g,x0}$, of the

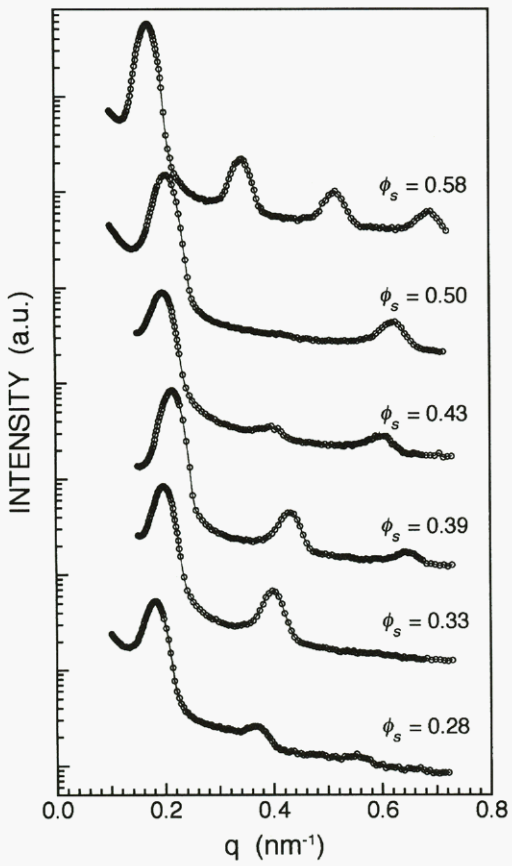

Figure 3. Comparison of SAXS edge-view diffraction patterns among samples with different polystyrene volume fractions. Samples are PSP-12, PSP-3, PSP-2, PSP-4, PSP-5, and PSP-14 from top to bottom.

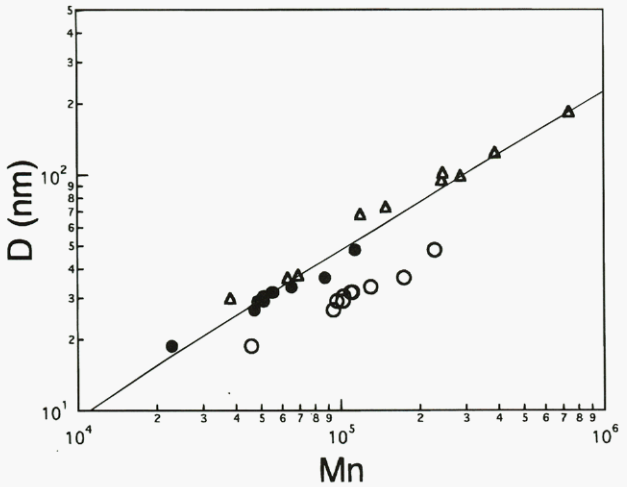

Figure 4. Domain spacing, D, versus the number-averaged molecular weight of samples, M_n, on a double logarithmic scale. The open circles are the data of PSP triblock copolymers while the filled circles denote the same data but they are plotted against $M_n/2$. The triangles are the data of SP diblock copolymers obtained in a previous work.[13]

middle block polystyrene and also the ratios $\alpha_x = R_{g,x}/R_{g,x0}$. $R_{g,x0}$'s were evaluated by using an empirical equation $R_{g,k0} = 0.0165M^{1/2}(nm)$,[22] where k is x, y, or z. It is apparent from this table that α_x decreases from unity with increasing molecular weight of polystyrene irrespective of the volume fraction and it also tends to increase with decreasing ϕ_s.

The degree of composition-matching was examined for two blends I and IV. Figure 7 compares two-dimensional intensity maps of PDP-5/PSP-11 blends with different mixing ratios in the edge view. The first and the second diffraction peaks are clearly observed along the horizontal axis in Figure 7a, which is for a blend with a weight percent of labeled block copolymer, w_L,

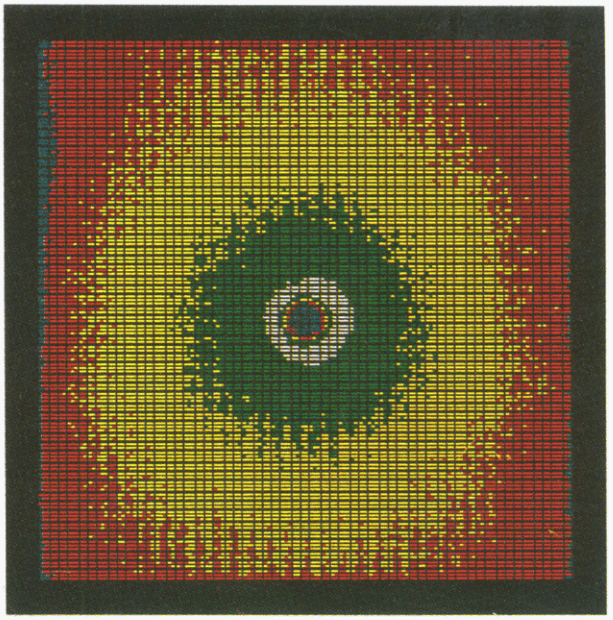

Figure 5. Typical isotropic intensity map on the two-dimensional detector for through-view measurement. Sample: PDP-5/PSP-11 (blend IV) with a blend ratio of 10.7/89.3 by weight. The sample to detector distance is 6 m.

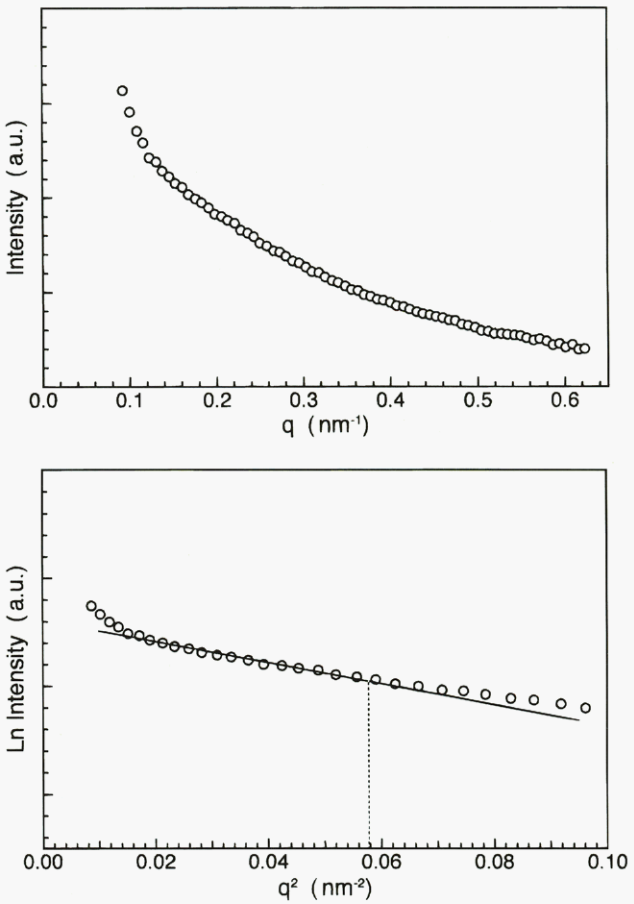

Figure 6. Example of circularly-averaged through-view coherent scattering intensities as a function of wave vector q (a) and their Guinier plots (b). The dotted vertical line in (b) indicates the limit of Guinier's range, i.e., $q^2R_g^2 \leq 1.3^2$ or $q^2R_{g,k}^2 \leq 1.3^2/3$, since $R_{g,k}^2 = R_g^2/3$.[17] Sample: blend IV.

Table 3. Chain Dimensions of Polystyrene Blocks and the Expansion Factors Relative to the Unperturbed Dimension

blend code	sample code	Φ_S	$R_{g,x}$	$R_{g,y}$	$R_{g,z}$	$R_{g,k0}$ ($k = x, y,$ or z)	α_x[a]	α_y[b]
I	PDP-1/PSP-8	0.32	2.48 ± 0.03	4.11 ± 0.13	2.48 ± 0.05	2.80	0.89 ± 0.01	1.47 ± 0.02
II	PDP-2/PSP-9	0.32	3.47 ± 0.07			4.12	0.84 ± 0.02	
III	PDP-4/PSP-10	0.51	2.30 ± 0.03			2.36	0.97 ± 0.01	
IV	PDP-5/PSP-11	0.50	3.12 ± 0.06	3.85 ± 0.05	3.25 ± 0.08	3.35	0.93 ± 0.02	1.15 ± 0.02
V	PDP-3/PSP-3	0.50	3.26 ± 0.07			3.53	0.92 ± 0.02	
VI	PDP-6/PSP-12	0.56	3.75 ± 0.05			4.31	0.87 ± 0.01	

[a] $\alpha_x = R_{g,x}/T_{g,x0}$. [b] $\alpha_y = R_{g,y}/R_{g,y0}$.

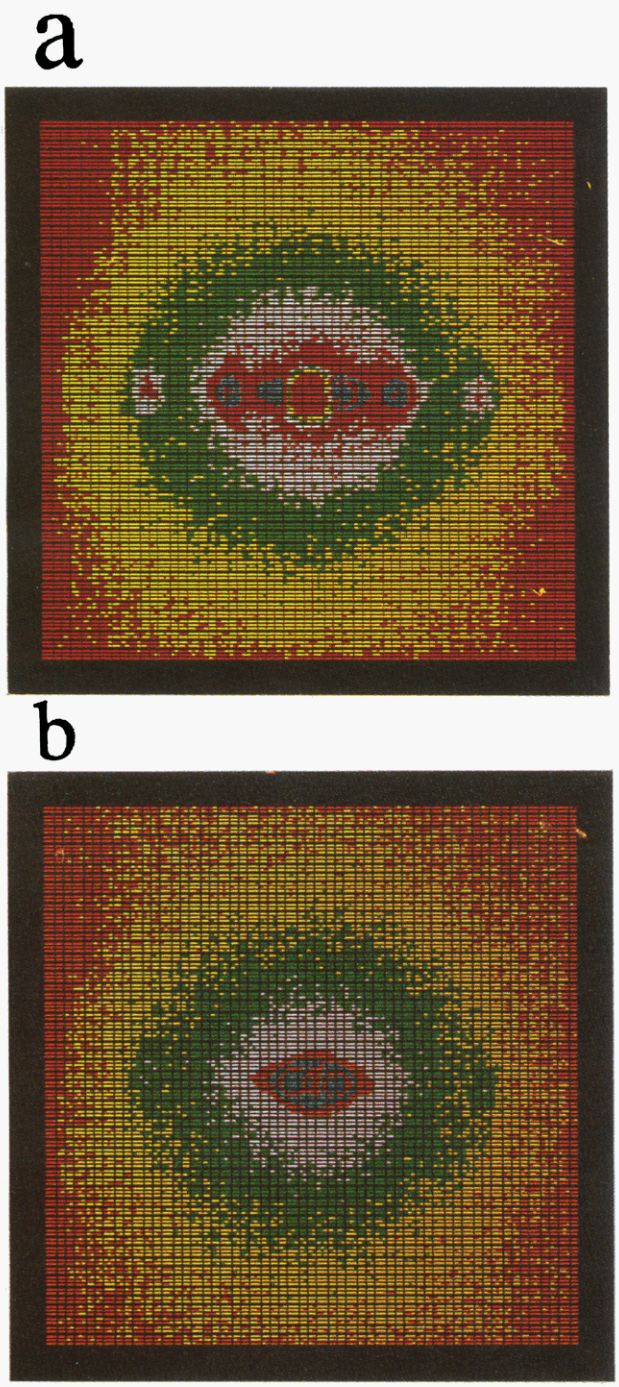

Figure 7. Comparison of edge-view two-dimensional maps of PDP-5/PSP-11 blends with different blend ratios, i.e., 13.0/87.0 (a) and 10.7/89.3 (b) by weight.

of 13.0%, whereas they disappear and only ansitropic scattering remains for a blend with a w_L of 10.7%, as shown in Figure 7b, reflecting the good achievement of composition-matching. Figure 8 compares the sum of the sector-averaged SANS intensities at $\psi = 0 \pm 5°$ and $180 \pm 5°$ for blend IV with various blend ratios. It is

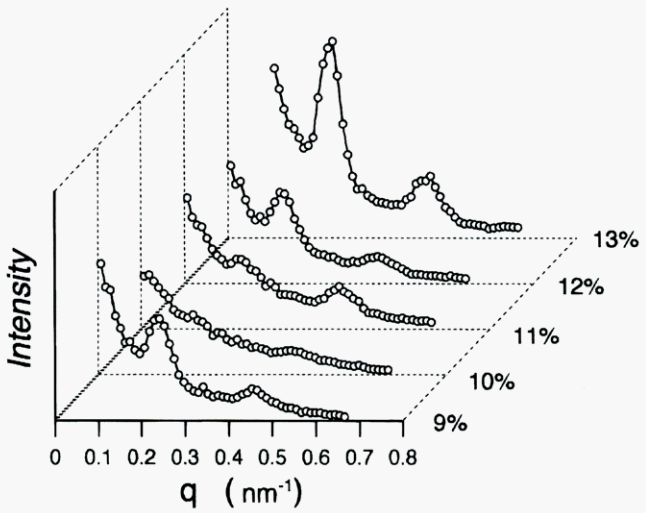

Figure 8. Variation of edge-view coherent scattering intensities with blend ratios. Sample: blend IV. The percentages along the third axis are for the labeled polymer.

apparent from this figure that the diffraction intensity decreases with increasing w_L up to 10% and then it turns to increase with further increasing w_L. The contrast factor, R, for diffraction between S and P domains in SANS is given by[23]

$$R = \frac{[\beta_P - x\beta_{SD} - (1 - x)\beta_{SH}]^2}{(\beta_P - \beta_{SH})^2} \quad (1)$$

where β_{SH}, β_{SD}, and β_P denote the coherent scattering length densities of hydrogenated polystyrene, deuterated polystyrene, and poly(2-vinylpyridine), respectively, and x is the volume fraction of the deuterated segment in the S domain. The experimental contrast factor R_e can be evaluated by

$$R_e = \Delta I(1)_x/\Delta I(1)_0 \quad (2)$$

where $\Delta I(1)_x$ and $\Delta I(1)_0$ are the sum of the sector-averaged diffraction intensities of the first-order peaks at $\psi = 0 \pm 5°$ and $180 \pm 5°$ for the blend sample with the volume fraction x and that for pure PSP block copolymers. The values R_e thus obtained are semilogarithmically plotted against x in Figure 9, where the dotted curve denotes eq 1 with 6.47, 1.41, and 1.95 × 10^{10} cm^{-2} for β_{SD}, β_{SH}, and β_P, respectively.[20] It is evident that the composition-matching is achieved reasonably well for the two blends, though the x values which give the minimum R_e are both a little smaller than the calculated value, i.e., 0.107.

Figure 10 compares Guinier plots of the sums of the edge-view intensities at $0 \pm 5°$ and $180 \pm 5°$ and at $90 \pm 5°$ and $270 \pm 5°$ for blend I with x of 0.102 and for blend IV with x of 0.101, where the minimum contrasts were attained. The radii of gyration along the y-axis, $R_{g,y}$ and along the z-axis, $R_{g,z}$, defined in Figure 1, were

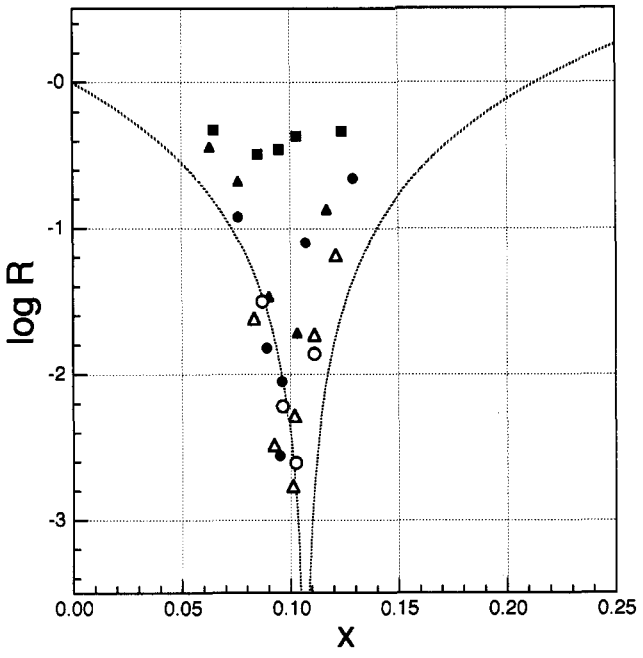

Figure 9. Contrast factor, R, as a function of the volume fraction, x, of the labeled segments in the polystyrene domain on a semilogarithmic scale. The open circles are for PDP-1/PSP-8 (blend I) and the open triangles are for PDP-5/PSP-11 (blend IV). The filled circles, triangles, and squares are for DP/SP diblock copolymer blends whose molecular weights of the labeled polystyrene block are 34K, 92K, and 162K, respectively.[20]

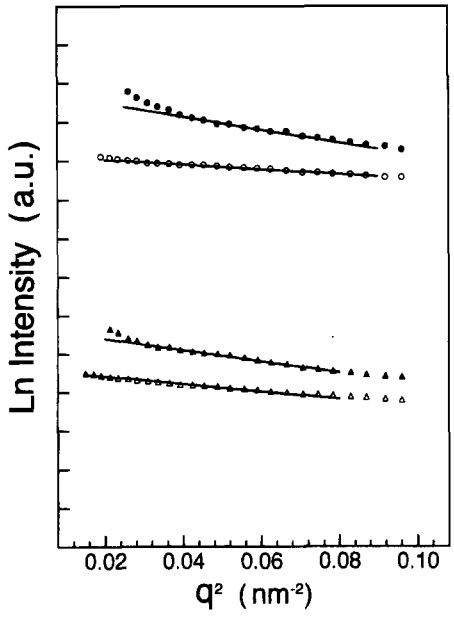

Figure 10. Guinier plots of the sector-averaged edge-view coherent scattering intensities. Circles are for blend I with x of 0.102, and triangles are for blend IV with x of 0.101. The filled symbols correspond to the data at 0 ± 5° plus 180 ± 5°, and the open symbols, to the data at 90 ± 5° plus 270 ± 5°.

evaluated from the initial slope of the data denoted by the filled and the open symbols for both blends, respectively. The radii of gyration, $R_{g,y}$ and $R_{g,z}$, thus obtained are also listed in Table 3. This table also lists the unperturbed radius of gyration $R_{g,y0}$ (=$R_{g,x0}$) and the ratios $\alpha_y = R_{g,y}/R_{g,y0}$. Figure 11 shows double logarithmic plots of $R_{g,x}$ and $R_{g,y}$ against the molecular weight of polystyrene, together with the data of diblock copolymers.[17] $R_{g,z}$ values are not plotted because $R_{g,x}$'s and $R_{g,z}$'s agree well with each other. Comparison between

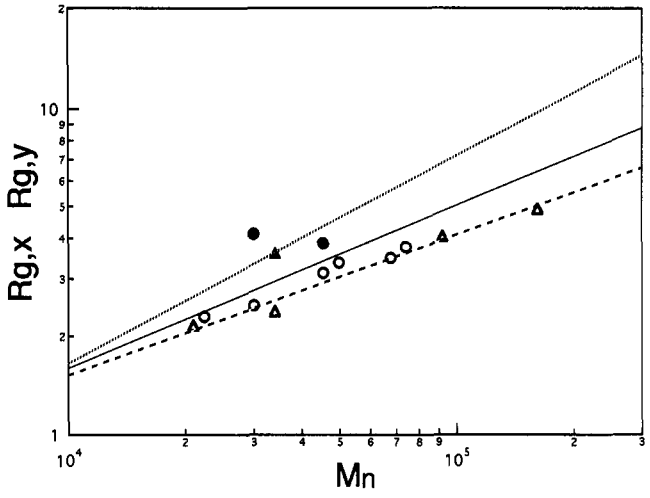

Figure 11. Double-logarithmic plots of the one-dimensional radii of gyration and the reduced number-averaged molecular weights of polystyrene blocks. Circles are for the present triblock copolymers, and triangles are for styrene−2-VP diblock copolymers reported in a previous work.[17] The open symbols are for $R_{g,x}$, and the filled symbols are for $R_{g,y}$. The solid line expresses the empirical equation $R_{g,\theta 0} = 0.0165M^{1/2}$ for the unperturbed polystyrene chains in bulk,[22] whereas the broken line and the dotted line denote the relationships $R_{g,x} = R_{g,z} = 0.289M^{0.43}$ and $R_{g,y} = 0.0453M^{0.64}$, respectively, which were determined experimentally from the data of styrene−2-VP diblock copolymers.[17]

blends I and IV in Table 3 reveals that α_y of the middle block, polystyrene, in blend I is much larger than that in blend IV, whereas α_x in blend I is smaller than that in blend IV; in other words, the chain conformation of polystyrene in blend I is more deformed than that in blend IV, even though the molecular weight of polystyrene in blend I is lower than that in blend IV.

Discussion

In Figure 4 the filled circles denote the lamellar domain spacings of ABA triblock copolymers plotted against half of the molecular weight $M_n/2$, and the solid line denotes the theoretical curve of symmetric diblock copolymers given by Helfand and Wasserman.[6]

$$-0.816\chi^{1/2}bN + D + 0.297D^{3.5}/(N^{1/2}b)^{2.5} = 0 \quad (3)$$

where N is the number of segments in a diblock copolymer, b is the statistical segment length of block polymers, and χ is the Flory−Huggins interaction parameter. Here we assumed $b = 0.68$ nm and $\chi = 0.08$ for styrene−2-VP diblock copolymers, as previously reported.[13] The data of the PSP triblock copolymers as well as SP diblock copolymers are in good agreement with the theoretical curve, even for the samples with the different volume fractions. This indicates that the lamellar domain spacings of ABA triblock copolymers are almost equal to those of diblock copolymers obtained by cutting the middle block at the center, as predicted by Helfand and Wasserman.[6]

In Figure 9 the degree of contrast-matching for PDP/PSP blends is compared with that for styrene−2-VP diblock copolymers.[20] In our previous paper we studied the contrast-matching between polystyrene and poly(2-VP) microdomains for blends of styrene-d_8−2-VP (DP) and styrene-h_8−2-VP (SP) diblock copolymers with 34K, 92K, and 162K for M_n of the poly(styrene-d_8) blocks. The study revealed that the contrast-matching between the two microdomains is reasonably well achieved only for

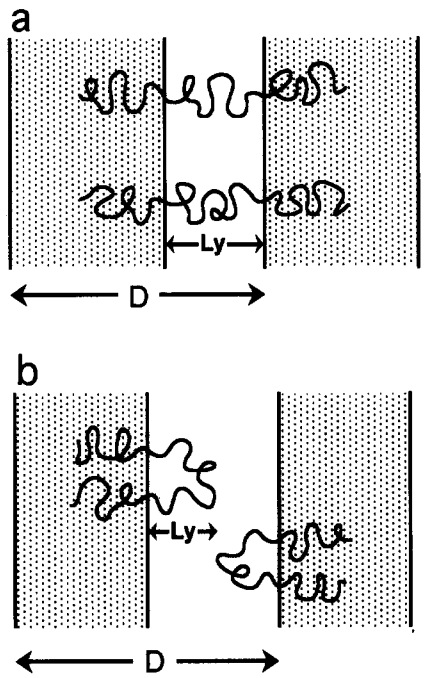

Figure 12. Schematics of chain conformations of triblock copolymers: (a) bridge-type conformation which is favorable for polymers with ϕ_S of $^1/_3$; (b) loop-type conformation which is favorable for polymers with ϕ_S of $^1/_2$.

the lowest molecular weight blends and the degree of matching evidently becomes worse if the molecular weight of the block chains increases. Hasegawa et al. also studied the contrast-matching between polystyrene (S) and polybutadiene (B) microdomains for butadiene-labeled (S−Bd) and -unlabeled (S−Bh) diblock copolymer blends,[25] and they found that it is not facile to match the contrast between two domains, whereas Quan and Koberstein[16] reported that contrast-matching between polystyrene and hydrogenated polybutadiene microdomains is reasonably well achieved to the extent that the diffraction peaks disappear by blending S−dB−S and S−hB−S triblock copolymers, where dB and hB denote deuterated and hydrogenated polybutadiene.

The above results imply that the phase-contrast-matching can be achieved more easily for ABA triblock copolymer blends than for AB diblock copolymer blends if the middle B block polymer of an ABA triblock copolymer is labeled and mixed with an unlabeled counterpart. This phenomena may be attributed to the contribution of the "bridge-type" conformation. Both ends of block chains with "bridge-type" conformation are anchored on the two different boundaries, so that we may consider that the segments of the block chains with this conformation are forced to distribute more uniformly along the y-axis than those of block chains with free ends, *even if the chain lengths between labeled and unlabeled blocks are different from each other*. Therefore, the scattering length density distribution made by a mixture of labeled and unlabeled segments is more uniform along the y-axis in the former than in the latter. Since the scattering length density profile along the y-axis is significant in the intensities at $0 \pm 5°$ and $180 \pm 5°$ in the edge-view experiments, the contrast-matching must be achieved more easily for chains with "bridge-type" conformation than those with free ends.

As described above, α_y of the middle block in blend I with the 1:1:1 composition for 2-VP, styrene, and 2-VP blocks or $\phi_S = ^1/_3$ is larger than that in blend IV with the 1:2:1 composition or $\phi_S = ^1/_2$. Figure 12 schematically shows the difference between "bridge-type" and "loop-type" conformations. If we assume that the domain sizes are proportional to the dimensions of block chains or the radii of gyration along the direction perpendicular to lamellae, we can estimate the radii of gyration along the y-axis for "bridge-type" and "loop-type" conformations by using the domain size−molecular weight relationships. Here, we use the theory of Semenov[8] for simplicity instead of the theory of Helfand and Wasserman since both theories agree with the data of diblock copolymers as previously reported.[13] As mentioned above, the lamellar domain spacings of ABA triclock copolymers are almost equal to those of diblock copolymers obtained by cutting the middle block at the center. If this approximation can be applied to the theory of Semenov,[8] the lamellar domain spacing (D) of ABA triblock copolymers with "loop-type" conformation is given by

$$D = (1/6)^{1/2}(48/\pi^2)^{1/3} b \chi^{1/6} N^{2/3} \quad (4)$$

where N is the number of segments in an ABA triblock copolymer. It is to be noted that this equation is equal to that of ABA triblock copolymers with "bridge-type" conformation if the chain conformation is the same as that of a block chain of a diblock copolymer. Since the free energy and hence the lamellar domain spacing do not depend on the composition, it is difficult to determine which type of conformation is favorable in terms of composition. *However, we have good reasons for speculating that the "loop-type" conformation is favorable for the molecular with a ϕ_B of $^1/_2$ and the "bridge-type" conformation is favorable for the molecule with a ϕ_B of $^1/_3$. Diblock copolymers have lamellar structures when ϕ_B values are around $^1/_2$, while ABC triblock copolymers, whose midblock chains must have "bridge-type" conformation, show lamellar structures when ϕ_B values are around $^1/_3$.*[26]

In our present PSP triblock copolymer case, if we can assume that the domain spacing (D) is proportional to the chain dimension along the y-axis, L_y, we have $L_y \propto D/4$ for the "loop-type" conformation of the triblock copolymer with $\phi_S = ^1/_2$ (Figure 12b) and $L_y \propto D/3$ for the "bridge-type" conformation when ϕ_S is $^1/_3$ (Figure 12a). Therefore, using eq 4, we have the ratio of the dimension along the y-axis of "bridge-type" to that of "loop-type", i.e., $L_{y,B}/L_{y,L} = (^1/_3)^{1/3}/(1/2)^{4/3} = (16/3)^{1/3} = 1.75$, if the molecular weights of the middle block polymers are the same. This value can be compared with the experimentally-obtained ratio of the radius of gyration along the y-axis, $R_{g,y}$, since $R_{g,y}$ may be proportional to L_y. Correcting for the molecular weight difference between polystyrenes in blends I and IV by assuming that the molecular weight dependence of $R_{g,y}$ is given by $R_{g,y} \propto M^{2/3}$, we have 1.37 for the ratio of the radius of gyration of polystyrene block in blend I to that in blend IV. *Since the experimental ratio is between 1 and 1.75, we conclude that the "loop-type" conformation is favorable for the molecule with a ϕ_S of $^1/_2$, while the "bridge-type" conformation is favorable for the molecule with a ϕ_S of $^1/_3$, as speculated, though in fact both molecules allow two conformations.*

To understand the contraction of middle block polymers in the direction parallel to lamellae, i.e., $\alpha_x < 1$, we compare the volumes of the deformed chain coils with those of the unperturbed coils, as reported previously.[17] Assuming that the segments in the deformed coil form an ellipsoid of revolution, of which the principal radii are proportional to the radii of gyration, $R_{g,y}$ and

Table 4. Estimation of Volumes Occupied by Polystyrene Blocks for Two Blends

blend code	$10^{-4} M_n$	ϕ_S	$V_d{}^a$ (nm^3)	$V_u{}^b$ (nm^3)
I	2.97	0.32	2.93[3]	2.84[3]
IV	4.43	0.50	3.39[3]	3.47[3]

[a] Volume of the deformed coil. [b] Volume of the unperturbed coil.

$R_{g,x}$ ($=R_{g,z}$), and the segments in the unperturbed coil form a sphere, of which the radius is proportional to the unperturbed radius of gyration, $R_{g0,k}$, the volumes of the deformed (V_d) and the unperturbed (V_u) coils are proportional to $R_{g,x}{}^2R_{g,y}$ and $R_{g0,k}{}^3$, respectively, where $k = x, y$, or z. As shown in Table 4 both volumes agree with each other irrespective of composition. Therefore, the more the block chain is extended in the direction perpendicular to lamellae, the more it is contracted in the parallel direction. This implies that the middle block polymers in ABA triblock copolymers are contracted so as not to change the degree of overlapping from the unperturbed state, irrespective of their chain conformations, similarly to block chains of diblock copolymers, as reported previously.[17]

Acknowledgment. This work was partially supported by a grant from The Daiko Foundation and Y. Matsushita is grateful to the support. The authors wish to thank Mr. H. Choshi for his help in preparing polymer samples. They also thank Mr. T. Watanabe and Mr. T. Imura in the glass blowing shop and Mr. S. Takahashi in the machinery shop at the school of Engineering of Nagoya University for their help in making cells and cell holders for SANS experiments.

References and Notes

(1) Present addresses: (a) Neutron Scattering Laboratory, The Institute for Solid State Physics, The University of Tokyo, Shirakata 106-1, Tokai-mura, Naka-gun, Ibaraki-ken, 319-11 Japan. (b) Toyota Motor Corp., 1, Toyota-cho, Toyota, Aichi, 471 Japan. (c) Fuji Photo Film Co., Ltd., Research Laboratories, Nakanuma 210, Minami-Ashigara, Kanagawa, 250-01 Japan. (d) Idemitsu Petrochemical Co., Ltd., Anegasaki1-1, Ichihara, Chiba, 299-01 Japan.
(2) Molau, G. E. In *Block Polymers*; Aggarwal, S. L., Ed.; Plenum Press: New York, 1970.
(3) Meier, D. J. In *Block and Graft Copolymers*; Burke, J. J., Weiss, V., Eds.; Syracuse University Press: Syracuse, NY, 1973.
(4) Inoue, T.; Soen, T.; Hashimoto, T.; Kawai, H. *J. Polym. Sci., Polym. Phys. Ed.* **1969**, *7*, 1283.
(5) Gallot, B. R. M. *Adv. Polym. Sci.* **1978**, *29*, 85.
(6) Helfand, E.; Wasserman, Z. R. *Macromolecules* **1976**, *9*, 881.
(7) Meier, D. J. *Polym. Prepr. (Am. Chem. Soc., Div. Polym. Chem.)* **1974**, *17*, 171.
(8) Semenov, A. V. *Soc. Phys. JETP (Engl. Transl.)* **1985**, *61* (*4*), 733.
(9) Ohta, T.; Kawasaki, K. *Macromolecules* **1986**, *19*, 2621.
(10) Hashimoto, T.; Shibayama, M.; Kawai, H. *Macromolecules* **1980**, *13*, 1237.
(11) Hadziioannou, G.; Skoulios, A. *Macromolecules* **1982**, *15*, 258.
(12) Richards, R. W.; Thomason, J. L. *Macromolecules* **1983**, *16*, 982.
(13) Matsushita, Y.; Mori, K.; Saguchi, R.; Nakao, Y.; Noda, I.; Nagasawa, M. *Macromolecules* **1990**, *23*, 4313.
(14) Hadziioannou, G.; Picot, C.; Skoulios, A.; Ionescu, M.-L.; Mathis, A.; Duplessix, R.; Gallot, Y.; Lingelser, J.-P. *Macromolecules* **1982**, *15*, 263.
(15) Hasegawa, H.; Hashimoto, T.; Kawai, H.; Lodge, T. P.; Amis, E. J.; Han, C. C. *Macromolecules* **1985**, *18*, 67.
(16) Quan, X.; Gancarz, I.; Koberstein, J. T.; Wignall, G. D. *J. Polym. Sci., Part B: Polym. Phys. Ed.* **1987**, *25*, 641.
(17) Matsushita, Y.; Mori, K.; Mogi, Y.; Saguchi, R.; Noda, I.; Nagasawa, M.; Chang, T.; Glinka, C. J.; Han, C. C. *Macromolecules* **1990**, *23*, 4317.
(18) Matsushita, Y.; Nomura, M.; Takabayashi, N.; Noda, I. Manuscript in preparation.
(19) Itoh, Y.; Imai, M.; Takahashi, S. *Physica B*, in press.
(20) Matsushita, Y.; Nakao, Y.; Saguchi, R.; Mori, K.; Choshi, H.; Muroga, Y. Noda, I.; Nagasawa, M.; Chang, T.; Glinka, C. J.; Han, G. C. *Macromolecules* **1988**, *25*, 641.
(21) Richards, R. W.; Thomason, J. L. *Macromolecules* **1983**, *16*, 982.
(22) Cotton, J. P.; Decker, D.; Benoit, H.; Farnoux, B.; Higgins, J.; Jannink, G.; Ober, R.; Picot, C.; des Cloizeaux, J. *Macromolecules* **1974**, *6*, 863.
(23) Koberstein, J. T. *J. Polym. Sci., Polym. Phys. Ed.* **1982**, *20*, 593.
(24) Takahashi, Y.; Matsushita, Y.; Noda, I.; Nakatani, A. I.; Kim, H.; Han, C. C. To be submitted for publication.
(25) Hasegawa, H.; Tanaka, H.; Hashimoto, T.; Han, C. C. *Macromolecules* **1987**, *20*, 2120.
(26) Mogi, Y.; Kotsuji, H.; Kaneko, Y.; Mori, K.; Matsushita, Y.; Noda, I. *Macromolecules* **1992**, *25*, 5408.

MA9463573